Pergamon

0301-9322(94)00092-1

*Int. J. Multiphase Flow* Vol. 21, No. 3, pp. 485–500, 1995
Copyright © 1995 Elsevier Science Ltd
Printed in Great Britain. All rights reserved
0301-9322/95 $9.50 + 0.00

# A CASCADE MODEL FOR NEUTRALLY BUOYANT DISPERSED TWO-PHASE HOMOGENEOUS TURBULENCE—II. NUMERICAL SOLUTION AND RESULTS

V. JAIRAZBHOY† and L. L. TAVLARIDES‡

Department of Chemical Engineering and Materials Science, Syracuse University, Syracuse, NY 13244, U.S.A.

*(Received 4 May 1992; in revised form 8 December 1994)*

**Abstract**—The two-phase cascade model for homogeneous, neutrally buoyant turbulent dispersions proposed earlier (Jairazbhoy *et al.* 1995 *Int. J. Multiphase Flow* **21**, 467–483) results in a system of partial integrodifferential equations. These are the energy, intermittency and population balance equations, and they account for the effects of drop–eddy interactions. A semi-discretization technique is developed for the solution. The drop number densities are discretized non-uniformly, the integrals approximated by Gaussian quadrature, and the resulting transient ODEs solved numerically to steady state using an integrator package. The results represent steady, isotropic turbulence with constant power input in the large eddies. The effects of phase fraction, drop size, Reynolds number and the model parameter on the turbulent spectrum and drop populations are examined. It is observed that the energy contained in large eddies is unaffected by drops, while small eddies are damped considerably. At low phase fractions, the energy spectrum is essentially unchanged by the dispersion. At high phase fractions, however, selective damping of the smaller eddies results in a sharp drop-off in the spectrum, tantamount to an increase in the apparent viscosity. The relative energy loss contributions from drop–eddy terms vary from about 8% for some cases with a phase fraction of 0.01 to over 82% in some instances with a phase fraction of 0.2. It is also found that, when the drops are too large to reside in a small eddy, the drop distribution in these eddies is substantially different from the overall distribution. Computation results comparing the energy spectra are in agreement with the model of Al Taweel & Landau at smaller and intermediate wave numbers, over which range comparisons are valid. These results suggest the model displays potential for the description of dense two-phase flows of breaking and coalescing drops, while accounting for drop interactions.

## 1. INTRODUCTION

In a previous paper (Jairazbhoy *et al.* 1995), it was observed that the mathematical modeling of turbulence in dense liquid dispersions of interacting drops poses numerous difficulties. Using a continuum framework for the mean flow, a two-phase cascade model was developed to describe the local turbulent energy spectrum, and hence the Reynolds stress term in the mean momentum balance. In the cascade model of Desnyansky & Novikov (1974) the spectrum is discretized, and an energy budget formulated for each discrete wave number. In the two-phase case, however, the number of eddies and the number of drops of each size are required for the estimation of their interaction frequencies. Hence, the Desnyansky & Novikov model was extended to include equations for the eddy intermittency and drop population distribution at each discrete wave number (Jairazbhoy 1989; Jairazbhoy *et al.* 1995). It was suggested that the interaction process in a dispersion can be viewed as a series of drop–drop (particle–particle) and drop–eddy (particle–fluid) collisions. The possible outcomes of interphase interaction processes were analyzed, and a set of drop–eddy events defined. The path of the droplet during these events was examined, and the effect on the three balances hence determined. On inclusion of the terms corresponding to the various interaction processes, the two-phase cascade model for homogeneous turbulence was

†Present address: Rm C130, Electronics Technical Center, Ford Motor Co., 17000 Rotunda Drive, Dearborn, MI 48121, U.S.A.
‡To whom correspondence should be addressed.

shown to take the following form:

$$\frac{du_n(t)}{dt} = \underbrace{\alpha k_n[u_{n-1}^2 - 2u_{n+1}u_n - 2^{1/3}C(u_{n-1}u_n - 2u_{n+1}^2)]}_{\text{I}} - \nu k_n^2 u_n$$

$$\underbrace{-\frac{1}{\rho_m u_n}[(\Delta E_E)_n + (\Delta E_T)_n + (\Delta E_S)_n + (\Delta E_B)_n + (\Delta E_D)_n]}_{\text{II}} + F\delta_{n1} \qquad [1]$$

$$\frac{d\beta_n(t)}{dt} = \underbrace{\beta_n v_n k_n[\log \beta_n - \log(\beta_{n-1}2^{D-3})]}_{\text{I}} - \underbrace{(\Delta\beta)_n}_{\text{II}} \qquad [2]$$

$$\frac{\partial N_n(v,t)}{\partial t} = \underbrace{-g_n(v)N_n(v,t) + \int_v^{(v_{\max})_n} v_n(v')\beta_n(v,v')g_n(v')N_n(v',t)\,dv'}_{\text{III}}$$

$$\underbrace{+\int_0^{v/2} \lambda_n(v-v',v')h_n(v-v',v')N_n(v-v',t)N_n(v',t)\,dv'}_{\text{III}}$$

$$\underbrace{+ F_s(v) + F_T(v) + F_D(v)}_{\text{II}} \qquad [3]$$

$$u_n(0) = u_n^0; \quad \beta_n(0) = \beta_n^0; \quad N_n(v,0) = N_n^0(v); \quad n = 1, \ldots, N \qquad [4]$$

The expressions marked (I), (II) and (III) refer to single-phase cascade, drop–eddy interaction and breakage and coalescence terms in the population balance, respectively. $F$ is the force of mode $n = 1$, required to sustain an equilibrium spectrum, and $\delta$ is the Kronecker symbol. $u_n$, $\beta_n$ and $N_n(v, t)$ are the $n$ eddy characteristic velocities, intermittencies and number densities, respectively. Here the term "$n$ eddy" refers to an eddy in the $n$th size range. The subscript $n$ refers to the $n$th discrete wave number, and takes values of $1, 2, \ldots, N$, where $N$ is the total number of discretization intervals. Also, in [1]–[3] $\alpha$ is a constant, $C$ is the reverse spectral transfer coefficient, $\nu$ is the kinematic viscosity, $k_n$ is the wave number of "$n$ eddies", $\rho_m$ is the density of the mixture, $v_n$ is a typical velocity of "$n$ eddies", $D$ is a similarity exponent, $g_n(v)$ is the breakage frequency of size "$v$" drops in "$n$ eddies", $\nu_n(v)$ are the number of daughter droplets formed due to breakage of a "$v$" volume drop in "$n$ eddies", $\beta_n(v, v')$ is the daughter drop distribution produced by breakage of a parent drop of volume of $v'$, $\lambda_n(v, v')$ is the collision efficiency between $v$ and $v'$ drops in "$n$ eddies", $h_n(v, v')$ is the collision frequency between $v$ and $v'$ drops in "$n$ eddies" and $(v_{\max})_n$ is the maximum volume of drops in "$n$ eddies". Several expressions in the terms marked (II) are Stieltjes integrals with limits that are functions of the dependent variables, $u_n$ and $\beta_n$. These terms are summarized in table 1 and are examined in more detail elsewhere (Jairazbhoy 1989). The form of the integrals is typically

$$I = \int_{(v_{do})_n}^{v_1} I_1\,dv_d + \int_{v_1}^{v_2} I_2\,dv_d + \int_{v_2}^{(v_{df})_n} I_3\,dv_d$$

Table 1. Summary of drop–eddy terms in a two-phase cascade model

| Equation No. | Term | Physical interpretation |
|---|---|---|
| [1] | $(\Delta E_E)_n$ | Energy lost due to grazing collisions |
| [1] | $(\Delta E_T)_n$ | Energy lost due to drop entrapment |
| [1] | $(\Delta E_S)_n$ | Energy lost due to eddy shattering |
| [1] | $(\Delta E_B)_n$ | Energy lost due to drop breakage |
| [1] | $(\Delta E_D)_n$ | Energy lost due to eddy turnover |
| [2] | $(\Delta\beta)_n$ | Intermittency sink term due to eddy shattering |
| [3] | $F_S(v)$ | Net increase of size $v$ drops due to eddy shattering |
| [3] | $F_T(v)$ | Net increase of size $v$ drops due to drop entrapment |
| [3] | $F_D(v)$ | Net increase of size $v$ drops due to eddy turnover |

where drop volumes $v_1$ and $v_2$ are functions of the eddy intermittencies and velocities. Integrands $I_1$, $I_2$ and $I_3$ are smooth over the range of integration and are functions of the drop number density functions and the eddy intermittencies and velocities.

This paper examines the numerical results of the partial integrodifferential equations [1]–[3] representing the two-phase cascade model for homogeneous turbulence. A semi-discretization procedure is used to solve the two-phase cascade model equations for specified initial conditions. The results presented in this paper are for drops that neither break nor coalesce. The effects of various system and model parameters on the steady-state energy and intermittency spectra, the local dispersed phase fraction, and the local drop size distribution are examined. The contribution of the dissipative particle–fluid terms in the energy equation [1] towards the total energy dissipated is also computed. The model is compared with others existing in the literature.

## 2. LITERATURE REVIEW

### *2.1. Studies on particle–turbulence interaction*

A number of studies have examined the effects of a particulate phase on the structure of turbulence (Kada & Hanratty 1960; Hjelmfelt Jr & Mockros 1966; Hetsroni & Sokolov 1971; Boothroyd & Walton 1973; Gore & Crowe 1989). They have observed that the viscosity, the integral scale, the turbulence intensity and viscous dissipation may all be affected. Kuchanov & Levich (1967) use a linearized particle equation of motion in a homogeneous, isotropic turbulent flow to determine a criteria for passive behavior of the mixture. Assuming Stoke's law, they develop an expression for the added energy dissipation in the presence of particles. Abramovich (1971) argues that in the process of turbulent fluctuating motion, fluid elements entrain foreign particles which are retarded under the action of drag, resulting in a decrease in the fluctuating velocity components of the flow. This argument resembles the rationale underlying the model presented in this paper.

The effect of particles on the turbulence intensity is noticeable only when the larger, energy-containing eddies are affected. Owen (1969) considers a dilute suspension with $t^* \ll t_e$ and obtains the energy dissipation in the presence of particles as

$$\epsilon = \epsilon_o\left(1 + \frac{\rho_p}{\rho}\right) \qquad [5]$$

where $t^*$ is the particle relaxation time, $t_e$ is the time scale of energy-containing eddies, $\epsilon_o$ is the turbulent energy dissipation rate in the absence of particles, $\rho$ is the density and $\rho_p$ is the mass of particulate phase per unit volume of dispersion. Further, assuming that the turbulence length scale is unaffected for a given mean velocity profile, Owen obtains

$$\frac{u'}{u'_o} = \left(1 + \frac{\rho_p}{\rho}\right)^{-1/2} \qquad [6]$$

where $u'$ and $u'_o$ are fluctuating velocity components in the presence and absence of particles, respectively.

Hinze (1971) identifies several indirect interaction effects resulting in modification of the fluid-velocity field in the interspace between the particles: (a) an effect due to increased shear rates; (b) an effect due to wakes of particles; (c) effects due to the fact that the continuous phase occupies less space; and (d) effects due to particle cluster formation. Hinze also discusses the "crossing trajectories" effect which could be interpreted as the migration of particles from one eddy to another. Although this effect is usually associated with non-neutrally buoyant particles (Snyder & Lumley 1971; Meek & Jones 1973; Calabrese & Middleman 1979; Chen 1983), Hinze (1971) observes that for a neutrally buoyant discrete particle, crossing trajectories may yield particle diffusivities which are slightly higher than the fluid diffusivity.

Al Taweel & Landau (1977) propose a model to predict the modification of the Kolmogoroff spectrum by a dispersed phase in two-phase jets. They attribute the "extra dissipation process" to the inability of particles to follow turbulent fluctuations completely. Assuming the particles to be uniformly distributed, they estimate the average rate of energy dissipation per unit mass of the fluid

resulting from interphase (particle–eddy) interactions. Their analysis shows that the attenuation of high frequency fluctuations increases with increasing particle loading and increases with increasing particle diameter. Also, turbulence intensities are reduced. The modulation of the turbulence spectrum is given by

$$\frac{E(k)_{TP}}{E(k)} = \exp\left[ -\frac{36\xi W\nu}{D^2\phi^1\epsilon_{TP}} \int_o^k \frac{R_k^2}{k^{5/3}} \right] \quad [7]$$

where $E(k)_{TP}$ and $E(k)$ are the two-phase and one-phase spectra, respectively, $\xi$ is an empirical constant, $W$ is the weight concentration of the dispersed phase, $\nu$ is the kinematic viscosity, $D$ is the particle diameter, $\phi^1$ is the density ratio, $\epsilon_{TP}$ is the two-phase energy dissipation rate and $R_k$ is the non-dimensional relative velocity. Although their study deals with non-neutrally buoyant suspensions, their philosophy and visualization of interphase interactions bear some resemblance to those in the present investigation.

Elghobashi & Truesdell (1992) perform a direct simulation to examine the interaction between small solid particles and decaying homogeneous turbulence. They solve the exact time-dependent, 3-D Navier–Stokes and continuity equations in a cubical domain with periodic boundary conditions. In addition, they track the instantaneous velocity of each particle by integrating the Langrangian equation of particle motion. Their results show that the particles increase the fluid turbulence energy at high wave numbers. This increase acts as a barrier to the energy cascade process from the low wavenumber range, and promotes extra dissipation at high wave numbers. The net result is a reduction in all the turbulence length scales, and hence a lower turbulent diffusivity of carrier fluid turbulence. These results cannot be compared directly with ours because of the respective limitations of the studies. Elghobashi & Truesdell documented the effect of very large density ratios of very small particles at very small phase fractions, whereas, our model allows large drop sizes, large phase fractions but is limited to neutrally buoyant drops.

## 3. SOLUTION, RESULTS AND DISCUSSION

A detailed discussion on solution methods for population balances and the specific solution scheme employed for [1]–[3] balance equations are presented elsewhere (Jairazbhoy 1989). To summarize, the scheme uses a semi-discretization procedure which bears resemblance to the method of Valentas & Amundson (1966), and to the method of lines which has proved to be efficient for the solution of partial differential equations (Liskovets 1965). The procedure also permits the use of Gaussian quadrature for accurate evaluation of integrals.

The number densities $N_n(v, t)$ are discretized using a successively-contained technique, compatible with a Gaussian quadrature scheme for the evaluation of the integrals. In some cases, Lagrange interpolation of the number densities is necessary for the calculation of these integrals. The resulting set of ordinary differential equations is solved by the integrator package EPISODEB (Byrne & Hindmarsh 1975). The major advantage of this method over that of Valentas & Amundson (1966) is that, for comparable accuracy, fewer discretization intervals are required. Therefore, fewer ODEs need to be solved. Also, EPISODEB provides more efficient integration than the predictor–corrector scheme used by Valentas & Amundson (1966). In addition, the non-uniform discretization permits a higher "density" of ODEs in the central region of the drop size distribution, and the quadrature weighting factors corresponding to integrals of the form specified in [1]–[3] can be chosen accurately. The disadvantage of the method is that the breakage and coalescence integrals in [3] have limits such that interpolation is required in the present scheme. If the method of Valentas & Amundson (1966) is used, interpolation of the number densities is unnecessary.

The semi-discretization of [1]–[3] results in a set of ordinary differential equations arranged in the following manner:

$$\frac{d\mathbf{H}}{dt} = \mathbf{G}(\mathbf{H}); \quad \mathbf{H}(o) = \mathbf{H}_o \quad [8]$$

where **G** represents the vector of functions describing the rate of change of $u_i$, $\beta_i$ and $N_{ij}$, $\mathbf{H}_o$ is the set of the initial values of the dependent variables, and **H** is the set of dependent variables arranged as follows:

$$\mathbf{H} = [u_1, \beta_1, N_{11}, \ldots, N_{1j}, \ldots, N_{1m}, \ldots, u_i, \beta_i, N_{i1}, \ldots, N_{ij}, \ldots, N_{im}, \ldots, u_N, \beta_N, N_{N1}, \ldots, N_{Nj}, \ldots, N_{Nm}]^T \quad [9]$$

where $N_{ij}$ is the descritized number density of $i$ eddies and $j$ sized drops. Equation [8] is solved numerically using the integrator package EPISODEB. For all runs carried out in this work, the variable-step variable order implicit Adams method with functional corrector iteration, suitable for non-stiff problems, is used. The relative error tolerance is tightened until no significant difference is observed in successive runs. The number of discretization intervals representing the number density is also increased until "grid-independence" is achieved for each run. The initial drop size distribution is calculated from the Chen–Middleman correlation (1967), normalized by the desired phase fraction. Care is taken to ensure that drops larger than the maximum permissible size in an $n$ eddy do not appear in these eddies. The starting values for $u_n$ and $\beta_n$ are taken from the solution of the single-phase cascade model. The set of equations in [8] is then integrated with a constant power input in the largest eddy, until steady state is achieved, simulating steady isotropic "turbulence in a box".

### *3.1. Effect of system and model parameters*

The effects of four parameters on the energy, intermittency and drop size distributions are studied. The parameters are (1) $N_{\mathrm{Re}}$, the Reynolds number based on large eddy properties calculated as $u_1/k_1\nu$, where $u_1$ and $k_1$ are the large eddy velocity and wave number, respectively; (2) $D_{32}$, the overall Sauter mean drop diameter; (3) $R_f$, the ratio of the maximum permissible radius of a drop in an $n$ eddy, to the parent eddy radius; and (4) $\phi$, the overall dispersed phase fraction.

The computations are carried out for three values of the Reynolds number—500, 1000, and 4000. Figures 1 and 2 present the energy and intermittency spectra for Reynolds numbers of 500 and 4000, respectively.

In both runs, the phase fraction is 0.1, the Sauter mean diameter is 1 mm, and the maximum dimensionless drop size $R_f$ is 0.4. The triangles represent the single-phase energy spectrum, which is used to generate initial values or the integration. The curve is virtually a straight line in the central part of the spectrum, with a slope of about $(-5/3)$—in agreement with the Kolmogoroff law. At a Reynolds number of 500 (figure 1), the smallest eddy size, indicative of the Kolmogoroff microscale, occurs at a wave number of 256 $m^{-1}$. At a Reynolds number of 4000 (figure 2), the wave number corresponding to the smallest eddies is 1024 $m^{-1}$. These eddies are comparable in size

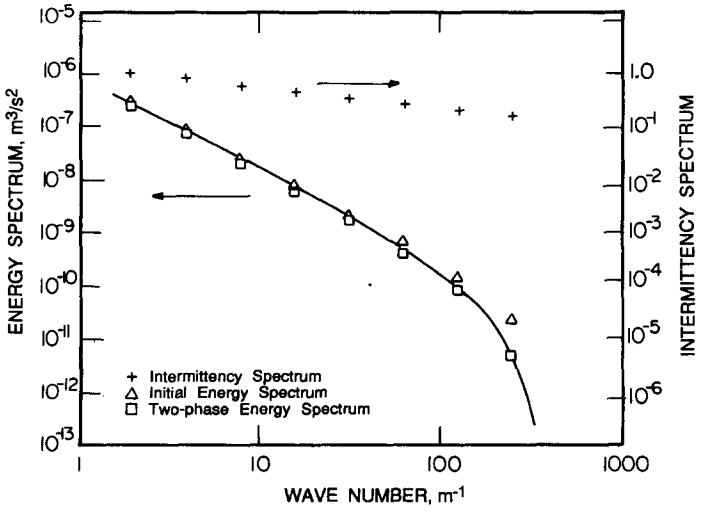


Figure 1. Energy and intermittency spectra for run 1: $N_{\mathrm{Re}} = 500$; $\phi = 0.1$; $D_{32} = 1.0$ mm; and $R_f = 0.4$.

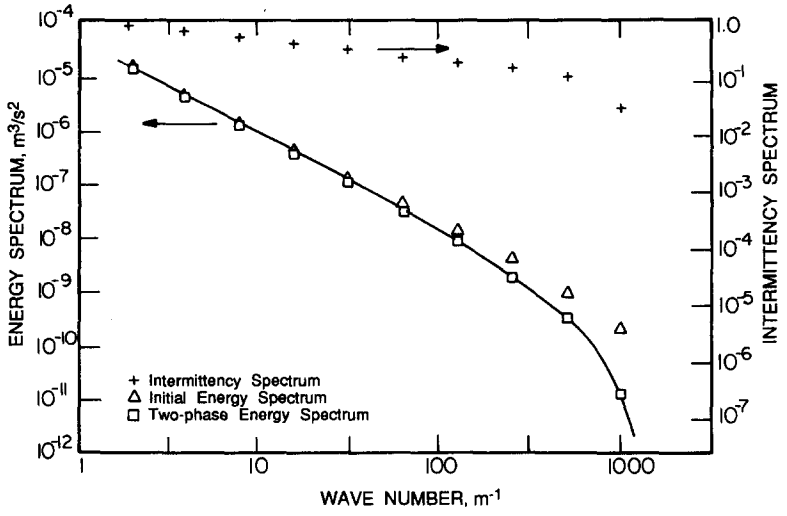


Figure 2. Energy and intermittency spectra for run 9: $N_{Re} = 4000$; $\phi = 0.1$; $D_{32} = 1.0$ mm; and $R_f = 0.4$.

to the drops ($D_{32} = 1$ mm) and are therefore susceptible to annihilation by drop–eddy collision (referred to as eddy shattering). Therefore, in figure 2, the intermittency factors at large wave numbers in the presence of droplets, represented by the symbol "+", fall off rapidly. This behavior indicates that a large fraction of the volume associated with the smallest eddies is not annihilated by collision. On the other hand, large eddies contain too much energy to succumb to destruction by shattering events. A similar trend is observed in the two-phase energy spectrum, depicted by the squares in figure 2. A sharp drop in the energy spectrum is observed at large wave numbers, indicating the presence of destructive drop–eddy collisions. At the smaller Reynolds number, however, the intermittency spectrum shows no drop-off, indicating that the smaller eddies have sufficient energy to withstand drop–eddy collisions.

The effect of the second phase on the lower end of the energy spectrum at a Reynolds number of 500, observed by comparing the squares with the triangles in figure 1, is less pronounced than at higher Reynolds numbers (figure 2). In both cases, the larger energy-containing eddies are essentially unaffected by the presence of drops, whereas the smaller eddies lose an observable amount of energy due to dissipative drop–eddy events. This steeper "cut-off" is tantamount to an increased apparent viscosity, i.e. a larger Kolmogoroff microscale, in agreement with prior observations (Hinze 1975). The overall dissipative effect of the drop–eddy interactions in figures 1 and 2, as a fraction of the total energy lost by viscous and drop effects, is shown in entries 1 and 9 of table 2. This fraction is calculated by dividing the dissipative energy contribution of the drop–eddy terms in [1] at steady state by the total power input to the system. It can be seen that at a higher Reynolds number, the relative drop–eddy energy losses are higher.

Table 2. Summary of computer runs and corresponding drop–eddy energy losses

| Run No. | Fig. Nos | $N_{Re}$ | $\phi$ | $D_{32}$ | $R_f$ | Relative drop–eddy losses (%) |
|---|---|---|---|---|---|---|
| 1 | 1 | 500 | 0.1 | 1.0 | 0.4 | 52.3 |
| 2 | — | 500 | 0.2 | 1.0 | 0.4 | 74.6 |
| 3 | — | 500 | 0.01 | 1.0 | 0.4 | 8.2 |
| 4 | 3, 5 | 1000 | 0.1 | 2.0 | 0.4 | 63.2 |
| 5 | 4, 6 | 1000 | 0.1 | 0.1 | 0.4 | 55.3 |
| 6 | 7, 8 | 1000 | 0.1 | 2.0 | 0.2 | 63.5 |
| 7 | 9 | 1000 | 0.2 | 2.0 | 0.4 | 82.5 |
| 8 | 10, 11 | 1000 | 0.01 | 2.0 | 0.4 | 11.9 |
| 9 | 2 | 4000 | 0.1 | 1.0 | 0.4 | 74.9 |
| 10 | — | 4000 | 0.1 | 0.1 | 0.2 | 67.9 |
| 11 | — | 4000 | 0.1 | 0.01 | 0.1 | 67.1 |
| 12 | — | 4000 | 0.1 | 1.0 | 0.1 | 64.0 |

For all runs: $\mu_c = 1$ cP; $\rho_c = 1000$ kg/m$^3$; $\rho_d = 1000$ kg/m$^3$.

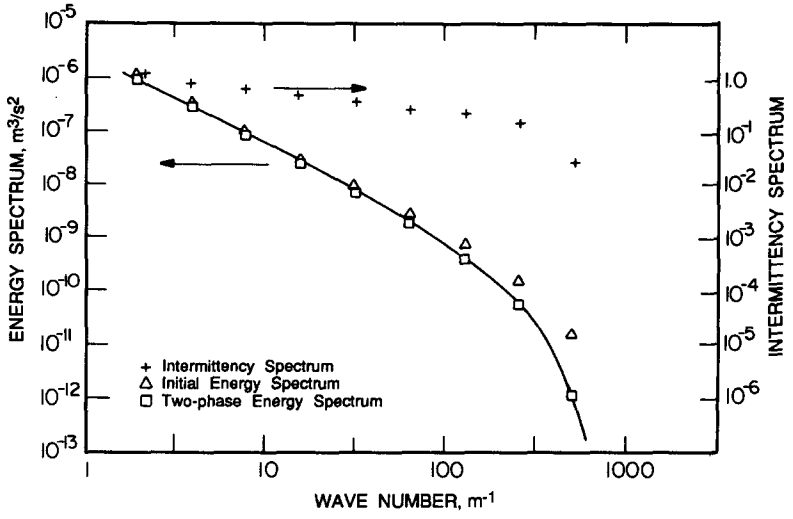


Figure 3. Energy and intermittency spectra for run 4: $N_{Re} = 1000$; $\phi = 0.1$; $D_{32} = 2.0$ mm; and $R_f = 0.4$.

Figures 3 and 4 indicate the effect of $D_{32}$ on the energy and intermittency spectra. In both cases the Reynolds number is 1000, $\phi$ is 0.1 and $R_f$ is 0.4. The large drop size in figure 3 ($D_{32} = 2$ mm) leads to annihilation of the smallest eddies, which shows up as a sharp drop-off in the intermittency spectrum. In figure 4, the drops are smaller with $D_{32} = 0.1$ mm. In this case, the drops do not have enough kinetic energy to cause disintegration of an eddy during a collision. Consequently, the eddy intermittency is unaffected by the drops. Examination of the single- and two-phase spectra in figures 3 and 4 reveals trends similar to those observed in figures 1 and 2. The second phase has a negligible effect on the large eddies, while a sharper "cut-off" is observed at the lower end of the two-phase spectrum. This cut-off is slightly steeper in the case of large drops, indicating that the drop–eddy effects are more prominent. This point is exemplified by entries 4 and 5 in table 2 in which the relative drop-eddy energy losses are seen to be about 8% higher for the case with large drops.

In addition to the possibility of eddy shattering in dispersions with large drops, the geometric limitation that large drops cannot reside within small eddies translates into preferential residence of large drops in large or mid-sized eddies. The result is that in figure 3 the drops of size 2 mm are subjected, on the average, to an environment which is somewhat different from that experienced by the drops of size 0.1 mm in figure 4. This argument is exemplified in figures 5 and 6, in which the "local" number densities associated with $n$ eddies, with $n$ taking the values 1, 4, 8 and 9, are

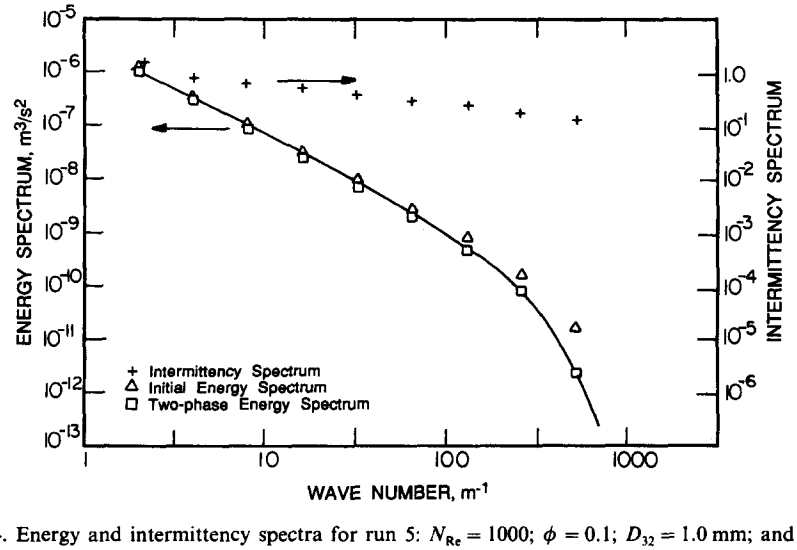


Figure 4. Energy and intermittency spectra for run 5: $N_{Re} = 1000$; $\phi = 0.1$; $D_{32} = 1.0$ mm; and $R_f = 0.4$.

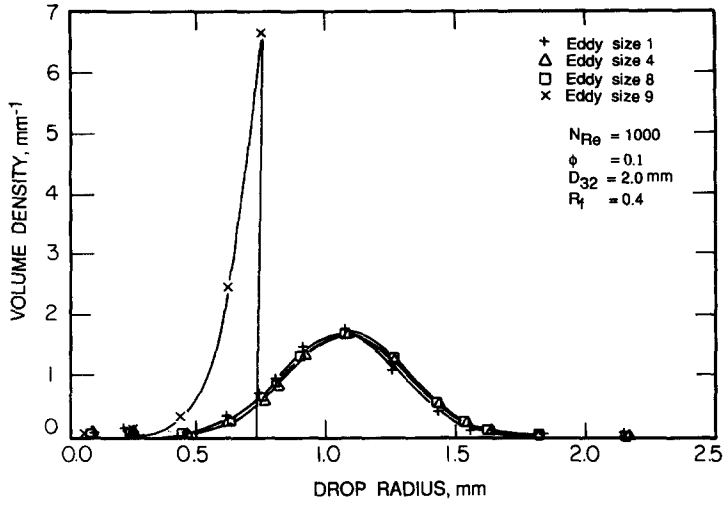


Figure 5. Number densities for run 4.

plotted for the two cases. For the case of large droplets, run 4 in table 2, the number densities for $n = 1, 4$ and 8 are very similar (figure 5). The smallest eddies ($n = 9$), however, look very different. The sharp cut-off is due to the prohibition of drops larger than a specified size. The results of run 5 in figure 6 show, however, that when the drops are much smaller than the Kolmogoroff microscale, the number densities associated with all four eddy sizes are identical, i.e. the four curves in figure 6 are superimposed. From table 3, however, the "local" phase fractions $\phi_n$ vary with the eddy size $n$. When the Sauter mean diameter is large, this trend is expected since a large section of drop distribution is prohibited from residing within the smallest eddies. Despite the small drop size, however, a significant variation in local phase fraction is observed in run 5. This observation is discussed later in this section.

From the above observations, two effects of drop size can be identified. First, the model predicts that large drops could annihilate the smaller eddies, and hence modify the turbulent structure and the drop environment. Second, geometric limitations prohibit large drops from residing in small eddies. Hence, the mean environment for these drops is somewhat different from that of sub-microscale droplets. The latter is in agreement with the observation that the motions of sub-microscale drops and drops in the inertial size range are driven by different mechanisms (Hinze 1975).

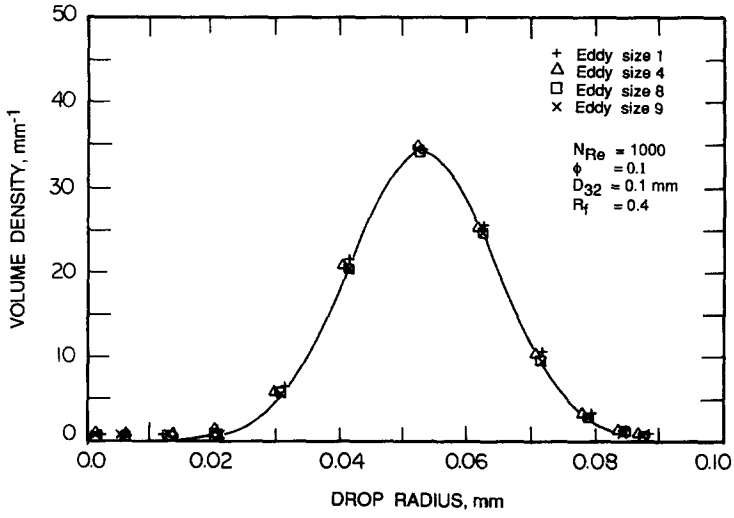


Figure 6. Number densities for run 5.

Table 3. Variation of local phase fraction and local mean drop size with eddy size

| Eddy size $n$ | Run 4 | | Run 5 | | Run 6 | |
|---|---|---|---|---|---|---|
| | $\phi_n$ (%) | $a_n$ (mm) | $\phi_n$ (%) | $a_n$ (mm) | $\phi_n$ (%) | $a_n$ (mm) |
| 1 | 9.3 | 1.06 | 9.3 | 0.053 | 10.9 | 1.06 |
| 2 | 9.4 | 1.06 | 9.4 | 0.053 | 11.0 | 1.07 |
| 3 | 9.7 | 1.06 | 9.5 | 0.053 | 11.2 | 1.07 |
| 4 | 10.0 | 1.06 | 9.7 | 0.053 | 11.5 | 1.07 |
| 5 | 10.7 | 1.06 | 10.0 | 0.053 | 12.2 | 1.07 |
| 6 | 12.1 | 1.06 | 10.5 | 0.053 | 13.8 | 1.07 |
| 7 | 15.7 | 1.07 | 11.5 | 0.053 | 17.0 | 1.07 |
| 8 | 11.8 | 1.07 | 14.0 | 0.053 | 2.0 | 0.67 |
| 9 | 1.4 | 0.68 | 12.4 | 0.053 | 0.33 | |

The maximum permissible dimensionless drop size $R_f$ is the only model parameter appearing in the modeling of the interphase interaction terms. This parameter has no effect if the drops are much smaller than the smallest eddy, as in run 5. A comparison of runs 4 and 6 (figures 3 and 7) shows the effect of changing $R_f$ from 0.4 to 0.2. A small difference is observed in the intermittency spectrum at large wave numbers, while the energy spectra remain virtually unchanged, as confirmed by the relative drop–eddy losses in table 2. In both cases, the eddy intermittency of the smallest eddies is affected by eddy shattering. In figure 7, however, the effect is less pronounced. The primary difference between the two cases lies in the drop distribution among the various eddy sizes, as observed from figures 5 and 8. The small value of $R_f$ in figure 8 has the effect of prohibiting large drops from the number densities of the two smallest eddy sizes. Only the number density of the smallest eddy size is modified in figure 5. This redistribution of drop sizes is likely to play a more significant role in the determination of the overall drop distribution in breaking and coalescing systems, since the rates of breakage and coalescence are determined by the turbulence properties of the embedding eddy. In the present case, however, the energy and intermittency spectra are fairly insensitive to the model parameter.

The overall phase fraction $\phi$ is the parameter which has the most significant effect on the energy spectrum. In runs 4, 7 (figure 9) and 8 (figure 10), the phase fractions are 0.1, 0.2 and 0.01, respectively. For $\phi = 0.01$, virtually no effects of the dispersed phase on the spectra are discernible. The relative drop–eddy loss from table 2 is barely 12%. For $\phi = 0.2$ in figure 9, the drop-off in the intermittency indicates that the smallest eddies are almost completely annihilated, and the two-phase energy spectrum indicates that they contain virtually no energy. All the effects are more pronounced, and the viscous cut-off is steeper. The relative eddy–drop loss from table 2 is 82.5% in run 7 as compared with 63.2% in run 4. The drop size distributions for all three runs, on the other hand, are virtually identical, as observed by comparing figures 5 and 11. This observation,

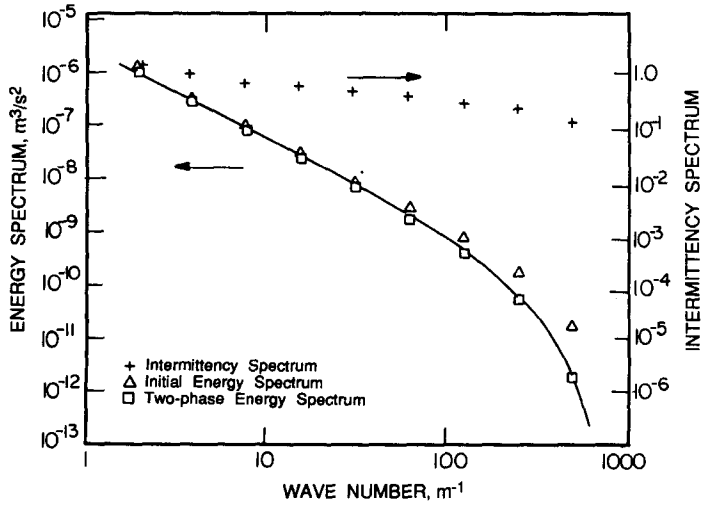


Figure 7. Energy and intermittency spectra for run 6: $N_{Re} = 1000$; $\phi = 0.1$; $D_{32} = 2.0$ mm; and $R_f = 0.4$.

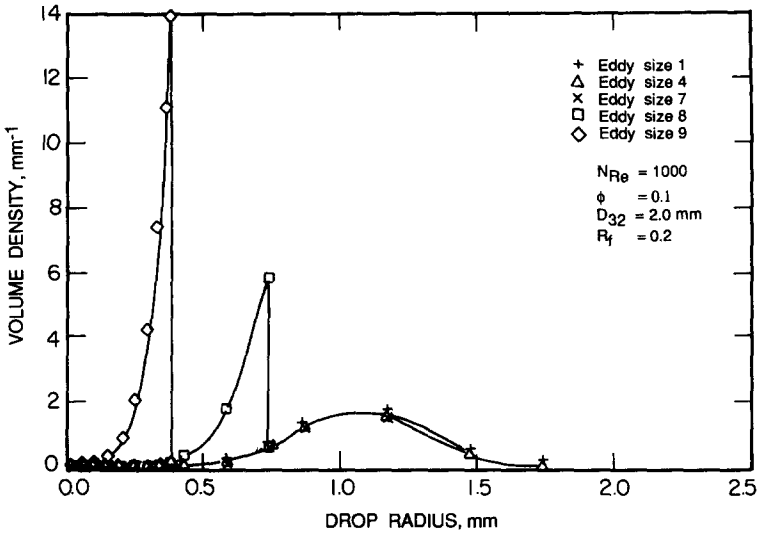


Figure 8. Number densities for run 6.

along with the number density plots in figures 6 and 8, suggest that the drop–eddy events of entrapment, exit, etc. do not seem to change the shape of the number density curve considerably, although they can have a significant effect on the local phase fraction $\phi_n$, and the energy and intermittency spectra.

On examining the results of the computer runs, a trend was observed in the variation of local phase fraction $\phi_n$ with the eddy size. Table 3 presents the local phase fractions of three separate runs. In all cases, $\phi_n$ undergoes a single maximum at the second or third smallest eddy size. In runs 4 and 6 a large fraction of the drops are larger than the maximum permissible in the smallest eddy. Due to this exclusion effect, the phase fraction in the smallest eddy is very low. In run 5 the drops are small, however, the exclusion effect is absent. The single maximum, however, still persists. Although this phenomenon could be an artifact of the model, the exclusion effect discussed earlier might play an important role in real systems by controlling the environment of the drop processes. Obviously, this effect also affects the mean drop size associated with the small eddies, as observed in table 3.

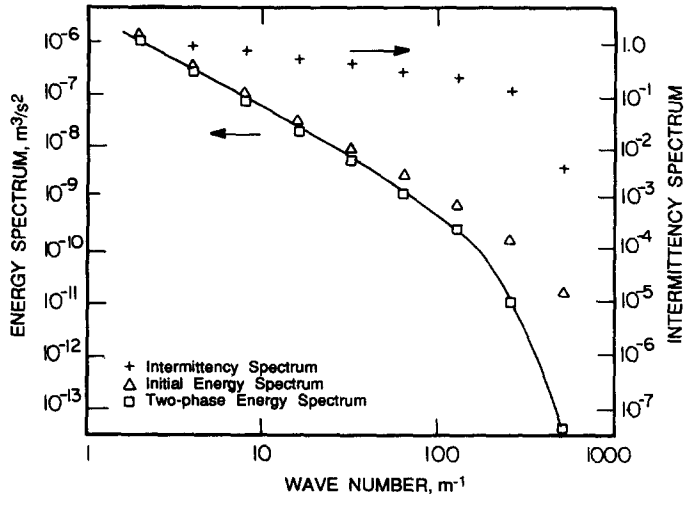


Figure 9. Energy and intermittency spectra for run 7: $N_{Re} = 1000$; $\phi = 0.2$; $D_{32} = 2.0$ mm; and $R_f = 0.4$.

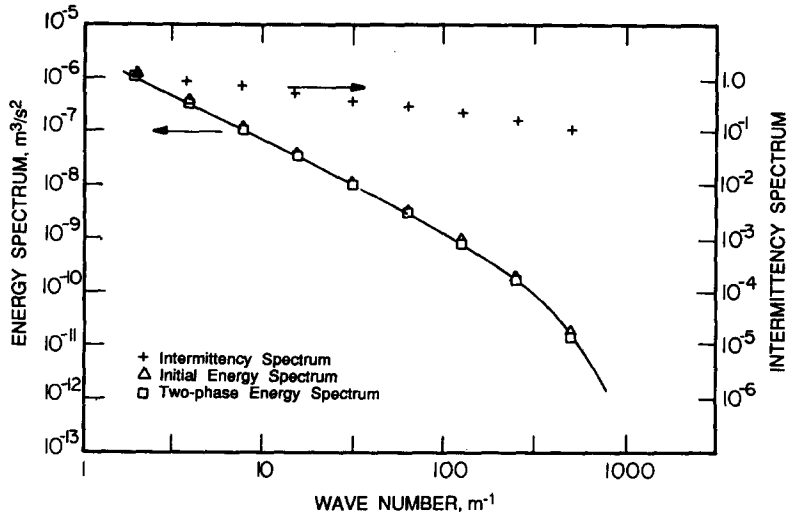


Figure 10. Energy and intermittency spectra for run 8: $N_{Re} = 1000$; $\phi = 0.01$; $D_{32} = 2.0$ mm; and $R_f = 0.4$.

### 3.2. *Comparison with previous studies*

The results presented here are in qualitative agreement with earlier work. A typical plot of the two-phase energy spectrum (e.g. figure 1) indicates that particle–fluid interactions modify the spectrum, especially at high wave numbers. This behavior has been noted by several authors (Lumley 1957; Meek & Jones 1973; Al Taweel & Landau 1977; Calabrese & Middleman 1979) and attributed to interaction phenomena such as crossing-trajectories and inertial effects. The former refers to the phenomena by which particles may not remain within a given region of correlated fluid but may instead migrate from one region to another. Although the crossing-trajectory effect is more dominant in non-neutrally buoyant suspensions with substantial free-fall velocity, Hinze (1971) observes that particle dispersion coefficients in neutrally buoyant suspensions can be greater than the fluid dispersion coefficients, and attributes this phenomenon to crossing-trajectories. As noted by Lumley (1957), the rate of energy cascading, determined by the slope of the energy spectrum in the inertial region, is essentially unchanged by the particles, whereas the high-frequency turbulence structure is damaged substantially.

Several authors have observed changes in local turbulence properties, such as turbulent kinetic energy, dissipation rate and eddy viscosity in the presence of particles (Lumley 1957; Kuchanov

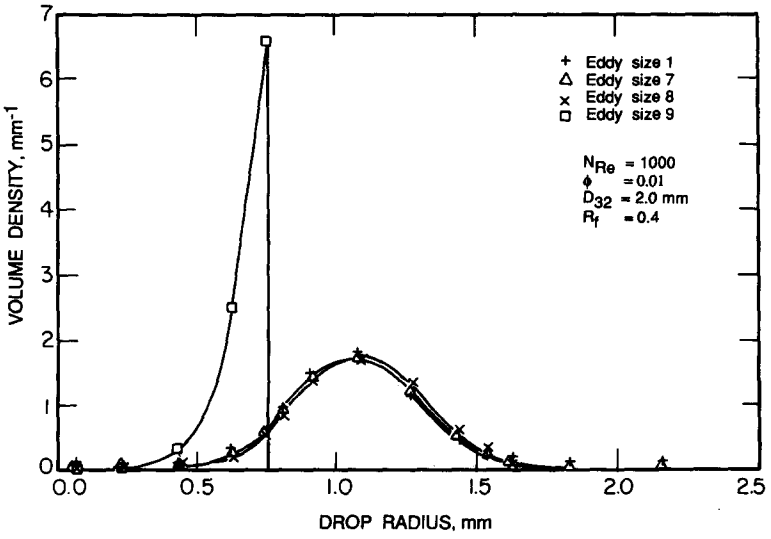


Figure 11. Number densities for run 8.

& Levich 1967; Abramovich 1971; Al Taweel & Landau 1977; Genchev & Karpuzov 1980). These authors note "additional dissipation" due to the presence of a dispersed phase. In the present study this added dissipation is determined by modeling interphase interactions, but the power input to the cascade, determined by the Reynolds number, is maintained at the same value for each pair of runs (single-phase and two-phase). Since energy is conserved in the cascade, the energy dissipated at steady state is the same for each pair. In practice, however, in order to maintain the same mean velocity in the presence of particles, greater power input (and hence energy dissipation) would be required. The kinetic energy of turbulence at a given power input, proportional to the area under the energy spectrum, is also seen to change in the presence of particles. These effects have been attributed to interaction phenomena such as (1) the entrainment and retardation by drag of foreign particles populating the fluid volume (Abramovich 1971; Genchev & Karpuzov 1980) and (2) the additional breakdown of eddies due to dust (Genchev & Karpuzov 1980).

The model development in the present work is similar to that of Lewalle *et al.* (1987). It is therefore instructive to compare the results of these two studies.

The results of Lewalle *et al.* (1987) indicate that large drops tend to exert a somewhat uniform damping effect spread over the lower and central regions of the spectrum, whereas tiny droplets, much smaller than the microscale, create a sharp drop in the energy at high wave numbers. In the present investigation, however, the drop size does not seem to affect the severity of the cut-off significantly. Small drops have a pronounced effect on the spectrum calculated by Lewalle *et al.* (1987) because the calculated drop–drop collision frequency, which is proportional to the square of the number of drops, is very large when the drops are small. Lewalle *et al.* (1987) also assume completely inelastic drop–drop collisions. Due to a combination of these effects, collisions between small drops contribute significantly towards the damping of the two-phase energy spectrum, especially in the high wave number range where the small eddies are particularly susceptible to dissipative interactions. A study of the relative velocity and the energy loss during collision in real systems would help resolve the actual effect of drop–drop interactions on the two-phase spectrum.

As observed earlier in this paper, the drop–eddy events incorporated in the model do not seem to affect the shapes of the local drop size distribution (e.g. figure 5). The number density curves resemble the Chen–Middleman volume density curve used for initialization of the overall density except for possible truncation due to the exclusion effect in the smaller eddies. Hence, in the absence of breakage and coalescence, it may be possible to represent the entire drop population by a single curve, and to determine the "local" number densities using the "local" intermittency and phase fraction. This procedure would require a method, perhaps a correlation, to determine the phase fractions associated with all eddy sizes. If this simplification can be achieved, no number density equations need be solved. As discussed earlier, the calculation of Lewalle *et al.* (1987) employs such a treatment. In the presence of breakage and coalescence, however, the "local" drop distributions are likely to vary with eddy size. In this case, the entire set of equations [1]–[3] would have to be solved. If the "shapes" of the distributions are similar, however, a single number balance for the entire population would be sufficient.

Due to a variety of difficulties in obtaining experimental data and the complicated nature of the theoretical problems, few studies have been conducted to examine the effects of a dispersed phase on the turbulent energy spectrum. Consequently, the authors could not find a study which offered a precise quantitative comparison for the two-phase cascade model. The models of Owen (1969) and Al Taweel & Landau (1977) do, however, provide some basis for comparison.

Owen bases his analysis on the assumption that, under certain conditions, the energy input to the turbulence is afforded entirely by the mean motion of the gas. In some sense, this situation is analogous to a two-phase turbulent energy cascade, with a fixed power input of magnitude as determined by the large eddy Reynolds number. Owen considers the case when $t^* \ll t_e$, where $t^*$ is the particle relaxation time and $t_e$ is the characteristic time of an energy containing eddy. Then, relative to the eddy, the particle will possess a motion only during a time comparable with $t^*$. In that period, assuming Stokes flow, the particle will be acted upon by a force

$$F = 3\pi\mu\, d_p u \qquad [10]$$

where $\mu$ is the viscosity, $d_p$ is the particle diameter and $u$ is the particle velocity. Owen then estimates the average rate of working during an eddy lifetime and the increase in the rate of turbulent energy dissipation, hence arriving at [5] and [6].

Equation [6] is used to calculate the kinetic energy of turbulence in the presence of a dispersed phase, for all the runs reported in this study. This quantity is compared with the predictions of the two-phase cascade model in figure 12. The predictions of the two models are within about 4% of each other.

Owen's model only yields a crude estimate of an integrated quantity—the kinetic energy of turbulence. As explained earlier, Al Taweel & Landau (1977) present a simple model to predict the modifying effect of a dispersed phase on the entire turbulent spectrum. Their model is based on Kolmogoroff's concept of spectral energy transfer and takes into account the additional energy dissipation resulting from the inability of the dispersed particles to follow the turbulent eddy fluctuations completely. It seems, however, that their model is applicable only when the primary cause of the relative velocity between the two phases is the density difference. Contrary to observation (c.f. Hinze 1971), the model predicts no effect of the dispersed phase on the turbulent structure in neutrally buoyant systems. The model seems applicable only in the regime in which density differences drive the relative motion between the phases. The authors apply the model effectively to describe gas–solid jets. No attempt is made to describe relative motion due to phenomena such as crossing trajectories. Their model could be used along with the two-phase cascade model, however, to examine the importance of density effects relative to the mechanisms postulated in this work and to provide a quantitative comparison for two-phase systems.

Figure 13 shows a typical comparison between three spectra calculated from: (a) the single-phase cascade model, (b) the two-phase cascade model and (c) the Al Taweel and Landau model. The two two-phase spectra are in close agreement at smaller and intermediate wave numbers but show significant differences in the large wave number range. This result is not unexpected since the Kolmogoroff spectrum, upon which the Al Taweel & Landau model is based, is not valid in the viscous sub-range.

To compare the importance of the particle–fluid interaction mechanisms postulated here against the density difference mechanism, the Al Taweel & Landau model was used to calculate two-phase turbulent kinetic energies for all computer runs reported in this work. The density ratio $\rho_d/\rho_c$ was adjusted in each run until the resulting kinetic energy was close enough to that calculated from the two-phase cascade model. Table 4 indicates those values of the density ratio. $\rho_d/\rho_c$ seems to be strongly correlated to the particle size, increasing as $D_{32}$ is decreased. For particles of size 2 mm, $\rho_d/\rho_c$ values lie between 2 and 2.5, while for particles of size 0.1 mm, $\rho_d/\rho_c > 10$. It could be inferred from this observation that (1) when the particles are extremely small, mechanisms unrelated to

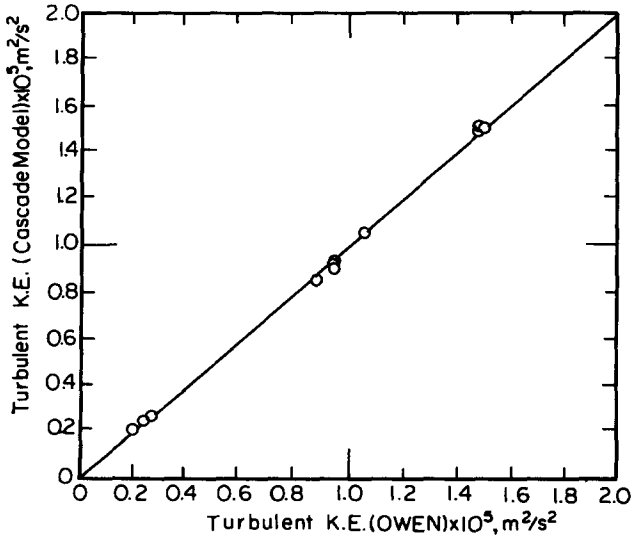


Figure 12. Turbulent kinetic energy—cascade model vs Owen's model.

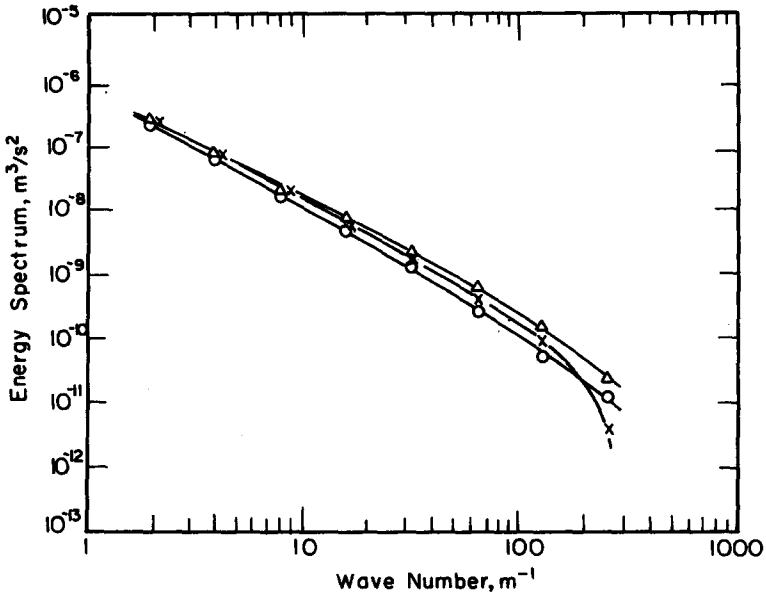


Figure 13. Comparison of energy spectra—cascade model vs model of Al Taweel & Landau [6]: Δ, single-phase cascade model; ○, Al Taweel & Landau model ($\rho_d/\rho_c = 4$); and ×, two-phase cascade model.

density differences determine the particle motion and hence the energy spectrum and (2) for solid–liquid or liquid–liquid systems with a density ratio of less than 2, density difference could play a secondary role in the two-phase spectrum.

As a final comparison, Elghobashi & Truesdell (1993) consider that the direct simulation of decaying turbulence with buoyant particles at very small phase fractions. Their calculated energy spectra exhibit some differences with our model results in that the effects of phase fraction, particle response time and particle diameter are not a simple monotone weakening of the energy spectrum. It is unclear whether this is a consequence of the finite time required for spectral transfer in a decaying field, or of a particle-mediated energy input to small eddies. More detailed results from similar large-scale computations may lead to modification of interphase dynamics in inexpensive models such as ours.

## 4. CONCLUSIONS

In this paper, the mutual interactions between a drop population and a homogeneous turbulent energy spectrum are studied by the analysis of numerical results from the solution of the two-phase cascade model equations. It is demonstrated that the simultaneous evolution of the drop number

Table 4. Comparison with the model of Al Taweel & Landau [6] (ATL model)

| Run No. | $N_{Re}$ | $\phi$ | $D_{32}$ | $R_f$ | $\rho_d/\rho_c$ in ATL model† | Dimensionless KE from cascade | Dimensionless KE from ATL model |
|---|---|---|---|---|---|---|---|
| 1 | 500 | 0.1 | 1.0 | 0.4 | 4.0 | 0.900 | 0.909 |
| 2 | 500 | 0.2 | 1.0 | 0.4 | 4.9 | 0.806 | 0.808 |
| 3 | 500 | 0.01 | 1.0 | 0.4 | 3.5 | 0.989 | 0.989 |
| 4 | 1000 | 0.1 | 2.0 | 0.4 | 2.2 | 0.893 | 0.881 |
| 5 | 1000 | 0.1 | 0.1 | 0.4 | 38.0 | 0.897 | 0.896 |
| 6 | 1000 | 0.1 | 2.0 | 0.2 | 2.2 | 0.880 | 0.883 |
| 7 | 1000 | 0.2 | 2.0 | 0.4 | 2.3 | 0.805 | 0.801 |
| 8 | 1000 | 0.01 | 2.0 | 0.4 | 2.0 | 0.988 | 0.990 |
| 9 | 4000 | 0.1 | 1.0 | 0.4 | 2.1 | 0.886 | 0.887 |
| 10 | 4000 | 0.1 | 0.1 | 0.2 | 10.5 | 0.887 | 0.890 |
| 11 | 4000 | 0.1 | 0.01 | 0.1 | 750.0 | 0.886 | 0.882 |
| 12 | 4000 | 0.1 | 1.0 | 0.1 | 2.2 | 0.872 | 0.873 |

†$\rho_d/\rho_c$ is adjusted until the two models give similar KE values.

density and the energy spectrum can be described by the model. A semi-discretization method is used to solve the two-phase cascade model equations for homogeneous, neutrally buoyant turbulent dispersions with no breakage or coalescence. The computational results show that the number densities local to eddies of a specific size bear resemblance to the overall number density, with the exception that large drops are not permitted in small eddies. The variation of the local phase fraction $\phi_N$ with $n$ displays a maximum, situated around the second or third smallest eddy. The relative energy loss contributions from drop–eddy terms in [1] vary from about 8% for some cases with a phase fraction of 0.01, to over 82% in some instances with a phase fraction of 0.2.

The integrodifferential equations solved in this study contain integrals with points of discontinuity in the integrands which are determined by the instantaneous values of the dependent variables. The set of equations also includes a partial integrodifferential population balance for each eddy size which contains feed and exit terms representing drop–eddy phenomena. The semi-discretization method employed gives rise to a set of ordinary integrodifferential equations which are solved simultaneously with the ordinary integrodifferential energy and intermittency equations by an integrator package.

The computational results are in agreement with previous studies on two-phase turbulence. From comparisons with the model of Al Taweel & Landau (1977), it could be inferred that if the particles are small (0.1 mm or less in diameter), or if the density ratio is much less than 2, mechanisms unrelated to density differences seem to determine particle motion and hence the two-phase energy spectrum.

## REFERENCES


Abramovich, G. N. 1971 Effect of solid–particle or droplet admixture on the structure of a turbulent gas jet. *Int. J. Heat Mass Trans.* **14,** 1039–1045.

Al Taweel, A. M. & Landau, J. 1977 Turbulence modulation in two-phase jets. *Int. J. Multiphase Flow* **3,** 341–351.

Boothroyd, R. G. & Walton, P. J. 1973 Fully developed turbulent boundary-layer flow of a fine solid–particle gaseous suspension. *Ind. Engng Chem. Fundam.* **12,** 75–82.

Byrne, G. D. & Hindmarsh, A. C. 1975 A polyalgorithm for the numerical solution of ordinary differential equations. *ACM Trans. Math. Software* **1,** 71–96.

Calabrese, R. V. & Middleman, S. 1979 The dispersion of discrete particles in a turbulent fluid field. *AIChE Jl* **25,** 1025–1035.

Chen, C.-P. 1983 Studies in two-phase turbulence closure modeling. Ph. D. dissertation, Michigan State University, MI.

Chen, H. T. & Middleman, S. 1967 Drop size distribution in agitated liquid–liquid systems. *AIChE Jl* **13,** 989–995.

Desnianskii, V. N. & Novikov, E. A. 1974 Simulation of cascade processes in turbulent flows. *J. Appl. Math. Mech.* **38,** 468–475.

Elghobashi, S. E. & Truesdell, G. C. 1992 Direct simulation of particle dispersion in a decaying isotropic turbulence. *J. Fluid Mech.* **242,** 655–700.

Elghobashi, S. E. & Truesdell, G. C. 1993 On the two-way interaction between homogeneous turbulence and dispersed solid particles. I: turbulence modification. *Phys. Fluids* **A5,** 1790–1801.

Genchev, Z. D. & Karpuzov, D. S. 1980 Effects of the motion of dust particles on turbulence transport equations. *J. Fluid Mech.* **101,** 833–842.

Gore, R. A. & Crowe, C. T. 1989 Effect of particle size on modulating turbulent intensity. *Int. J. Multiphase Flow* **15,** 279–285.

Hetsroni, G. & Sokolov, M. 1971 Distribution of mass, velocity, and intensity of turbulence in a two-phase turbulent jet. *J. Appl. Mech.* **June,** 315–327.

Hinze, J. O. 1975 *Turbulence*, 2nd edn, p. 461. McGraw–Hill, New York.

Hinze, J. O. 1971 Turbulent fluid and particle interaction. In *Progress in Heat and Mass Transfer* (Edited by Hetsroni, G., Aideman, S. & Hartnett, J. P.), Vol. 6, pp. 433–452. Pergamon Press, Oxford.

Hjelmfelt, A. T. Jr & Mockros, L. F. 1966 Motion of discrete particles in a turbulent fluid. *Appl. Sci. Res.* **16,** 149–161.

JAIRAZBHOY, V. 1989 An analysis of the two-phase flow of turbulent dispersions. Ph.D. dissertation, Syracuse University, Syracuse, NY.

JAIRAZBHOY, V., TAVLARIDES, L. L. & LEWALLE, J. 1995 A cascade model for neutrally buoyant dispersed two-phase homogeneous turbulence—I. Model formulation. *Int. J. Multiphase Flow* **21,** 467–483.

KADA, H. & HANRATTY, T. J. 1960 Effects of solids on turbulence in a fluid. *AIChE Jl* **6,** 624–630.

KUCHANOV, S. I. & LEVICH, V. G. 1967 Energy dissipation in a turbulent gas containing suspended particles. *Sov. Phys. Dokl.* **12,** 549–551.

LEWALLE, J., TAVLARIDES, L. L. & JAIRAZBHOY, V. 1987 Modeling of turbulent, neutrally buoyant droplet suspensions in liquids. *Chem. Engng Commun.* **59,** 15–32.

LISKOVETS, O. A. 1965 The method of lines (review). *Diff. Equations* **1,** 1308–1323.

LUMLEY, J. L. 1957 Some problems connected with the motion of small particles in turbulent fluid. Ph.D. thesis, Johns Hopkins University, Baltimore, MD.

MEEK, C. C. & JONES, B. G. 1973 Studies of the behavior of heavy particles in a turbulent fluid flow. *J. Atmos. Sci.* **30,** 239–244.

OWEN, P. R. 1969 Pneumatic transport. *J. Fluid Mech.* **39,** 407–431.

SNYDER, W. H. & LUMLEY, J. L. 1971 Some measurements of particle velocity autocorrelation functions in a turbulent flow. *J. Fluid Mech.* **48,** 41–71.

VALENTAS, K. J. & AMUNDSON, N. R. 1966 Breakage and coalescence in dispersed phase systems. *Ind. Engng Chem. Fund.* **5,** 533–542.